

## PICTORIAL REVIEW

# Müllerian duct anomalies: from diagnosis to intervention

T M CHANDLER, MD, L S MACHAN, MD, P L COOPERBERG, MD, A C HARRIS, MD and S D CHANG, MD

Department of Radiology, University of British Columbia, 3350–950 West 10th Avenue, Vancouver, BC V5Z 4E3, Canada

**ABSTRACT.** The purpose of this study was to review the embryology, classification, imaging features and treatment options of Müllerian duct anomalies. The three embryological phases will be described and the appearance of the seven classes of Müllerian duct anomalies will be illustrated using hysterosalpingography, ultrasound and MRI. This exhibit will also review the treatment options, including interventional therapy. The role of imaging is to help detect, classify and guide surgical management. At this time, MRI is the modality of choice because of its high accuracy in detecting and accurately characterising Müllerian duct anomalies. In conclusion, radiologists should be familiar with the imaging features of the seven classes of Müllerian duct anomalies, as the appropriate course of treatment relies upon the correct diagnosis and categorisation of each anomaly.

Received 14 October 2008

Revised 22 January 2009

Accepted 27 January 2009

DOI: 10.1259/bjr/99354802

© 2009 The British Institute of Radiology

Müllerian duct anomalies (MDA) are uncommon but can be a treatable form of infertility [1]. Patients with MDA are known to have higher incidences of infertility, repeated first trimester spontaneous abortions, fetal intra-uterine growth retardation, fetal malposition, pre-term labour and retained placenta [1]. The role of imaging is to detect and classify these MDA so that appropriate treatment is undertaken.

### Embryology

The female reproductive tract develops from a pair of Müllerian ducts that form the following structures: fallopian tube, uterus, cervix and the upper two-thirds of the vagina. The ovaries and lower third of the vagina have different embryological origins derived from germ cells that migrate from the primitive yolk sac and the sinovaginal bulb, respectively.

Normal development of the Müllerian ducts depends on the completion of three phases: organogenesis, fusion and septal resorption. Organogenesis is characterised by the formation of both Müllerian ducts. Failure of this results in uterine agenesis/hypoplasia or a unicornuate uterus. Fusion is characterised by fusion of the ducts to form the uterus. Failure of this results in a bicornuate or didelphys uterus. Septal resorption involves subsequent resorption of the central septum once the ducts have fused. Defects in this stage result in a septate or arcuate uterus.

### Classification system

It is important to classify MDA properly because the associated risks of poor pregnancy outcome and treat-

ment can vary widely between anomalies [1] (Table 1). The most common classification system is that developed by the American Society of Reproductive Medicine [1] (Figure 1). It is important to realise that this classification system is merely a framework and that not all anomalies will fit completely into one of the categories. In situations where a case does not fit into a category, it is more important to accurately describe the component parts than to artificially place it into a category that doesn't fully describe it.

### Imaging modalities

Hysterosalpingography (HSG) allows for assessment of the uterine cavity and tubal patency but is limited at visualising the external uterine contour. Ultrasound is quick, readily available, economical and lacks radiation. However, image degradation can occur with large patients, overlying bowel gas, and the external contour may be difficult to visualise. Three-dimensional (3D) ultrasound is a new technique that has shown, in experienced hands, to be more accurate than two-dimensional ultrasound and equal or better than MRI at assessing MDA [2]. 3D ultrasound has the potential of becoming the imaging standard for MDA [2]. However, MRI is currently considered the best imaging modality for MDA. It lacks radiation and provides clear delineation of both the internal and the external uterine anatomy. MRI has been shown to have excellent agreement with the clinical diagnosis of the subtypes of MDA [3].

### Class I — agenesis/hypoplasia

Early developmental failure of the Müllerian ducts, for unknown reasons at around 5 weeks' gestation, results in various degrees of agenesis or hypoplasia of the uterus, cervix and upper two-thirds of the vagina. In agenesis

Address correspondence to: Silvia D Chang, Department of Radiology, Vancouver General Hospital, 899 West 12th Avenue, Vancouver, BC V5Z 1M9, Canada. E-mail: Silvia.Chang@vch.ca

**Table 1.** Summary of the therapeutic interventions performed for the different classes of Müllerian Duct anomalies

Class	Treatment
<b>I – Hypoplasia/agenesis</b>	No reproductive potential; medical intervention in the form of <i>in vitro</i> fertilisation of harvested ova and implantation in a host uterus needed
<b>II – Unicornuate</b>	
Non-communicating, cavitary horn	Always surgically resected, as it is associated with dysmenorrhoea, haematometra, endometriosis and ectopic pregnancy
Non-communicating, non-cavitary horn	Surgery not currently recommended. No complications of endometriosis etc, as there is no endometrium
Communicating, cavitary horn	Also surgically removed because pregnancy that implants in the rudimentary horn rarely is viable
No horn	No treatment. Reproductive potential is possible
<b>III – Didelphys</b>	May consider metroplasty; however, full-term pregnancies have occurred
<b>IV – Bicornuate</b>	Surgical intervention rarely needed; may consider metroplasty
<b>V – Septate</b>	Often treated with transvaginal hysteroscopic resection of the septum. Conception is possible 2 months after surgery

(Figure 2), a uterus is not identified or small amounts of rudimentary tissue without differentiation may be present. The most common form is the Mayer–Rokitansky–Kuster–Hauser syndrome. This consists of a combined agenesis of the uterus, cervix and upper portion of the vagina. Symptoms may manifest at puberty as primary amenorrhoea with normal secondary sexual characteristics, as ovarian function is preserved. The ovaries originate within the primitive ectoderm and not from the paramesonephros, and thus these patients have normal female sexual development. In uterine hypoplasia, a small but fully differentiated organ is present.

**Class II — unicornuate**

This anomaly results from complete or near-complete arrested development of one of the Müllerian ducts

(Figures 3 and 4). Four possible subtypes can develop: (i) absent rudimentary horn, (ii) non-cavitary (non-functional) rudimentary horn, (iii) cavitary communicating rudimentary horn and (iv) cavitary non-communicating rudimentary horn. The last one may obstruct and present with abdominal pain, subsequently requiring surgical intervention.

**Class III — didelphys**

This anomaly results from complete non-fusion of both Müllerian ducts (Figures 5 and 6). The individual horns are fully developed and almost normal in size. A deep fundal cleft and two cervixes are present. A longitudinal or transverse vaginal septum may be present.

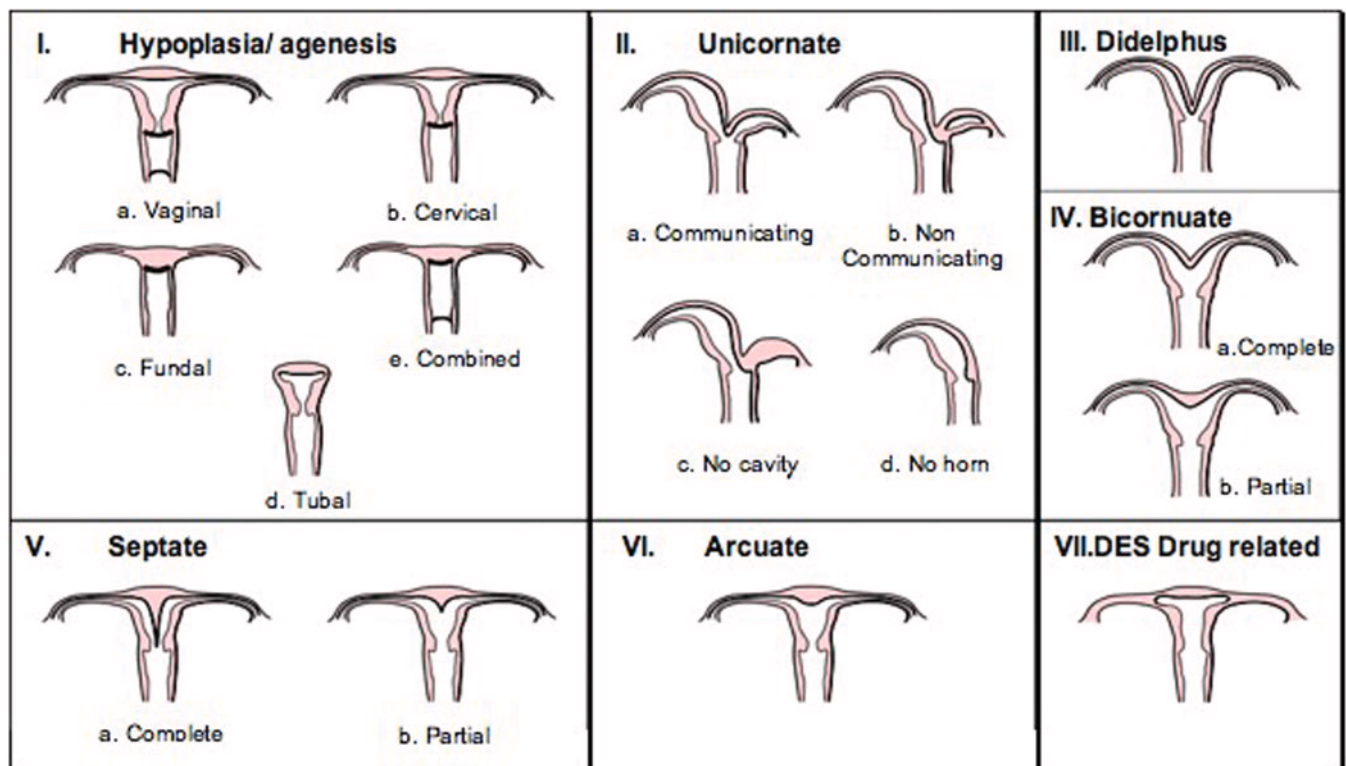


**Figure 1.** The classification system of Müllerian duct anomalies used by the American Fertility Society.

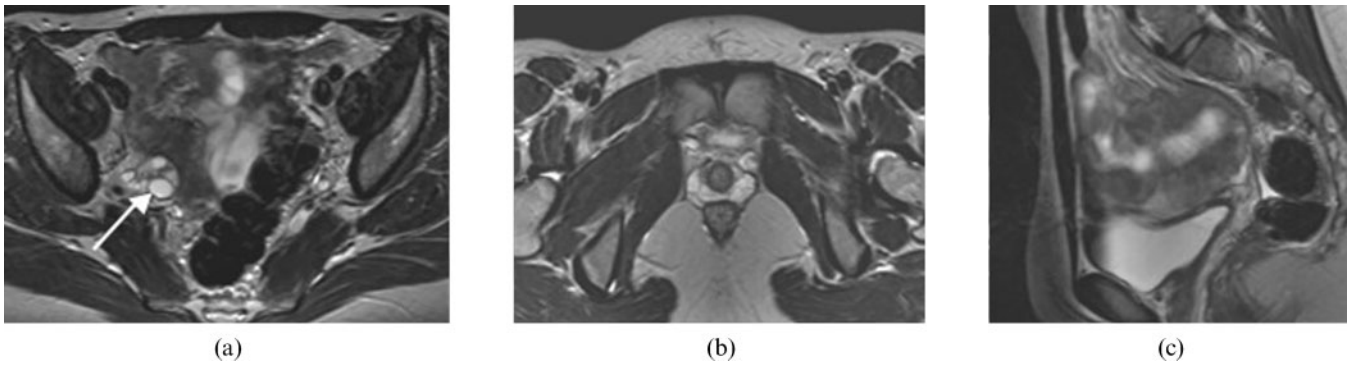


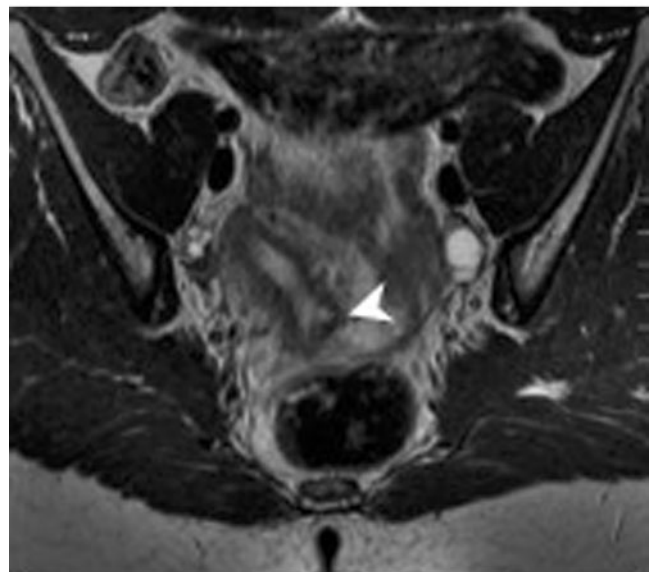
**Figure 2.** A 19 year-old woman with uterine and vaginal agenesis (Class I). (a,b) Axial and (c) sagittal  $T_2$  MRI of the pelvis demonstrates normal ovaries (arrow depicts the right ovary; left not shown) and absent uterus and upper vagina consistent with Mayer-Rokitansky-Kuster-Hauser syndrome. Note the ovaries are not visualised in (b,c).



(a)

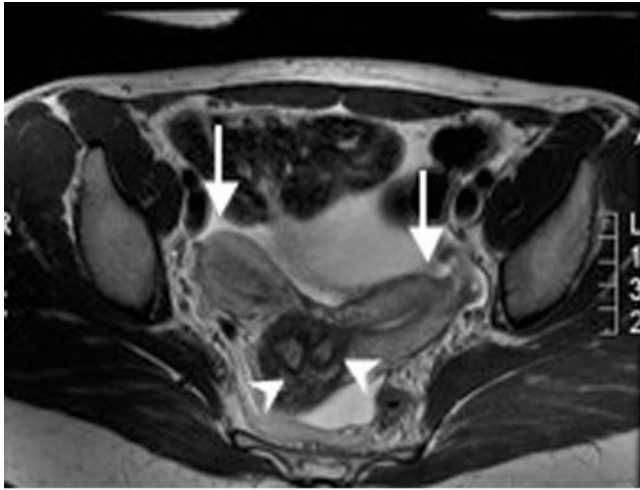


**Figure 3.** A 22-year-old woman with a unicornuate uterus with no rudimentary horn (Class II). Axial  $T_2$  weighted MRI illustrates the classic banana shape appearance of the unicornuate uterus (arrow).

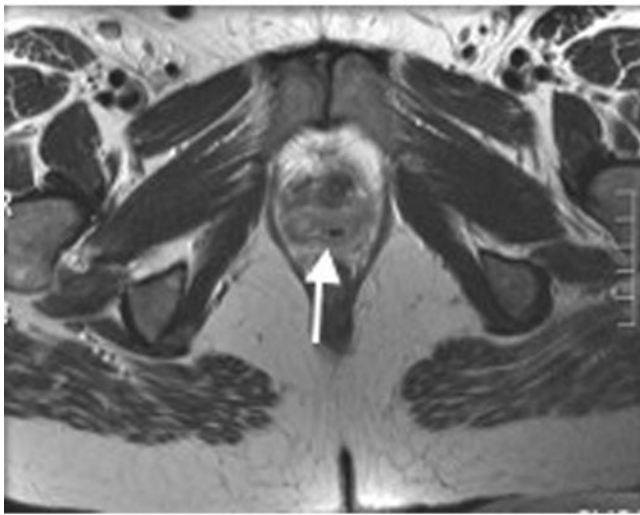


(b)

**Figure 4.** A 29-year-old woman with a unicornuate uterus and a rudimentary horn (Class II). (a) Hysterosalpingogram reveals a unicornuate uterus (arrow) with a rudimentary communicating horn (arrowhead). (b) Correlative axial  $T_2$  weighted MRI confirms that there is no obstructing component beyond the patent rudimentary horn (arrowhead).



(a)



(b)

**Figure 5.** A 26-year-old woman with uterus didelphys (Class III). (a) Axial  $T_2$  weighted MRI demonstrating complete duplication of the uterine horns (arrows) and cervixes (arrowheads). (b) A septum (arrow) dividing two vaginal canals.

#### Class IV — bicornuate

This class is characterised by partial non-fusion of the Müllerian ducts (Figure 7). This results in a central myometrium that may extend to the level of the internal cervical os (bicornuate unicollis) or external os (bicornuate bicollis), with a fundal cleft  $>1$  cm deep. The horns of the bicornuate uteri are not as fully developed and are smaller than those in the didelphys uteri.

#### Class V — septate

This class of anomaly occurs when the final fibrous septum between the two Müllerian ducts fails to resorb. This results in the formation of a uterus that is completely or partially divided into two cavities (Figures 8–10). The septum may be muscular (with similar signal intensity as the myometrium) [2], fibrous or a combination of both. This class is associated with the

poorest obstetrical outcomes [4]. It is important to distinguish a fibrous septum from a muscular septum, as the former can be repaired by a hysteroscopic approach, whereas the latter may require a transabdominal surgical approach. The fundal cleft is  $<1$  cm deep [5] and the intercornual distance is usually  $<4$  cm. The morphology of the outer fundal contour is the key to the diagnosis. The differentiation between a septate and bicornuate uterus is important because they differ in their reproductive prognosis and treatment (Table 1).

#### Class VI — arcuate

This group is characterised by mild indentation of the endometrium at the uterine fundus (Figure 11a,b). It is the result of near complete resorption of the uterovaginal septum. Currently, no definitive depth has been established to differentiate the arcuate configuration from the septate. This class is highly controversial, as it remains unclear whether this variant should be classified as a true anomaly or as an anatomic variant of normal. Data regarding the reproductive outcome of patients in this category are extremely limited and conflicting. Currently, it is generally thought that an arcuate uterus is compatible with normal pregnancy and delivery.

#### Class VII — diethylstilbestrol related

Several million women were treated with diethylstilbestrol (DES), a non-steroidal oestrogen, to prevent miscarriage between 1945 and 1970 [6]. The drug was promptly removed from the market when it was found that up to 15% of newborn girls who were exposed to DES had uterine malformations and an increased risk of vaginal clear cell carcinoma [6]. The uterine abnormalities include hypoplasia and a T-shaped uterine cavity (Figure 12). Patients may also have abnormal transverse ridges, hoods and stenoses of the cervix.

#### Association with renal anomalies

Renal anomalies occur in 29% of MDA [7] and are more commonly associated with unicornuate uteri than with other MDA [7]. They are reported in roughly 40% of unicornuate patients and are ipsilateral to the rudimentary horn [7]. Renal agenesis is the most commonly reported anomaly, occurring in 67% of cases [7] (Figure 13). Other anomalies include ectopic kidney, horseshoe kidney, renal dysplasia and duplicated collecting systems.

#### Interventional radiology

Interventional radiology (IR) has been used in some selected cases in combination with a hysteroscopy approach [8] (Figure 14). IR may be used as the primary therapeutic procedure, such as in the case of a failed laparoscopic-assisted resection of a non-communicating horn. In this case, an ultrasound-guided needle is advanced into the cavity and dilatation of the tract is

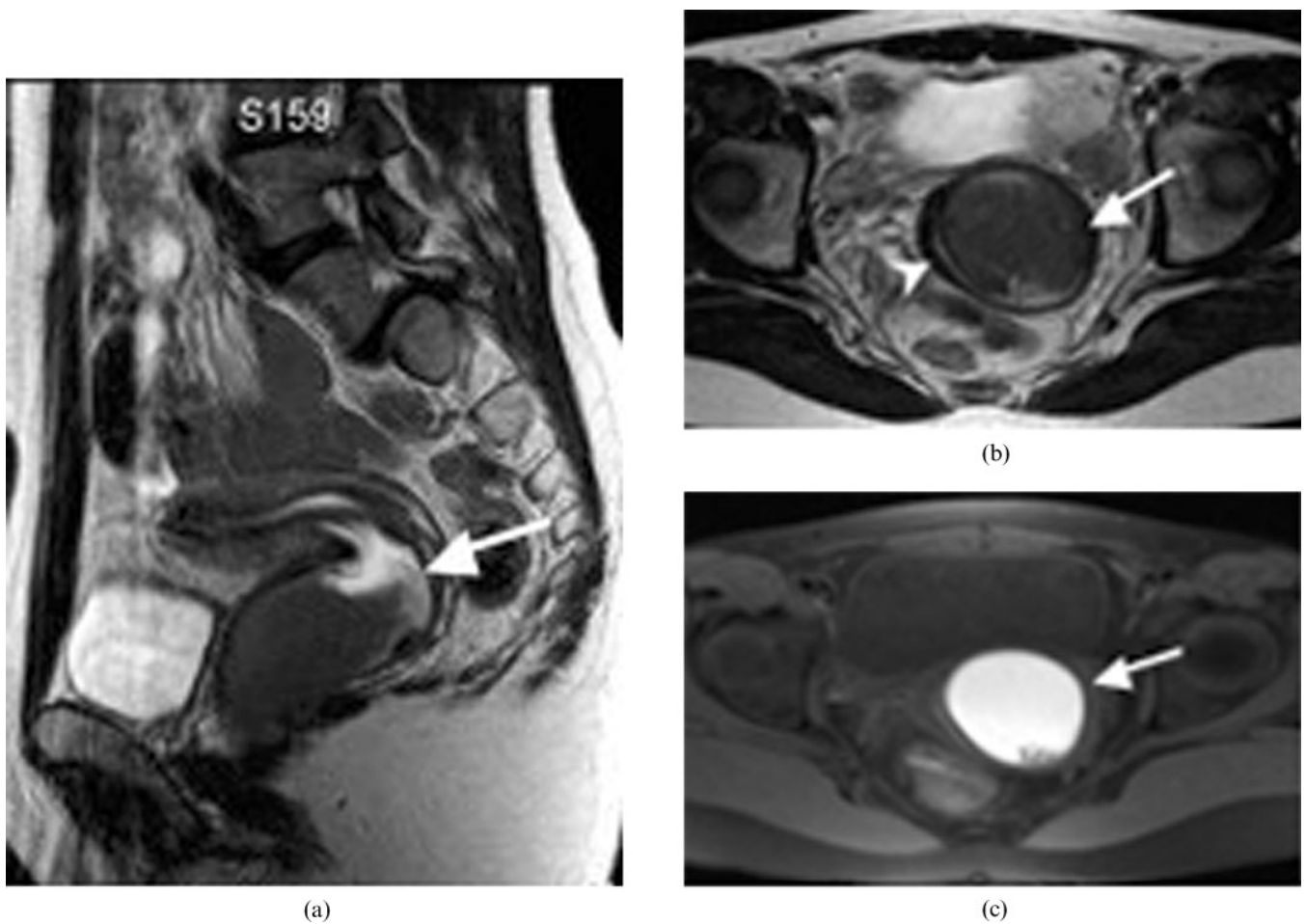


**Figure 6.** A 19-year-old woman with didelphys uterus (Class III). (a) Sagittal  $T_2$  weighted MR image of a didelphys uterus with a transverse vaginal septum causing unilateral haematocolpos (arrow). (b) Axial  $T_2$  weighted MR image shows a dilated left vaginal canal with predominantly low signal intensity fluid (arrow) and compressed right vaginal canal (arrowhead). (c) Correlating axial  $T_1$  weighted fat saturation MR image shows hyperintense fluid in the distended left vaginal canal in keeping with haematocolpos (arrow).

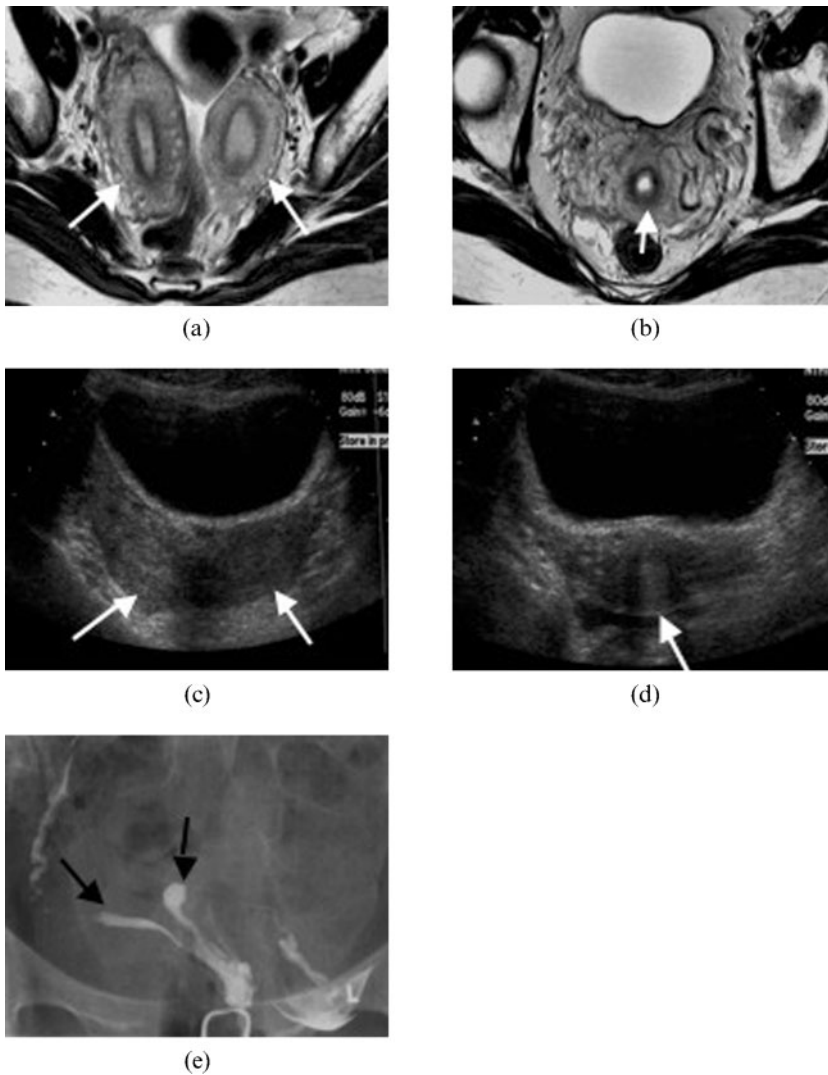


**Figure 7.** A 30-year-old woman with a bicornuate uterus (Class IV). Axial  $T_2$  weighted image illustrating (a) two separate uterine horns (arrows) that fuse at its inferior end to give (b) a single cervix (arrow). Transverse ultrasound images demonstrating (c) two uterine horns (arrows) and (d) a single cervix (arrow). (e) Hysterosalpingography of a bicornuate uterus. The contrast material fills two separate uterine horns (arrows).

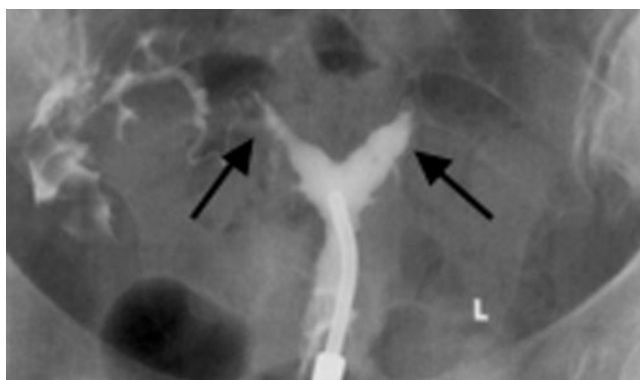


**Figure 8.** A 32-year-old woman with a septate uterus (Class V). Hysterosalpingography demonstrates that there are two uterine horns (arrows).

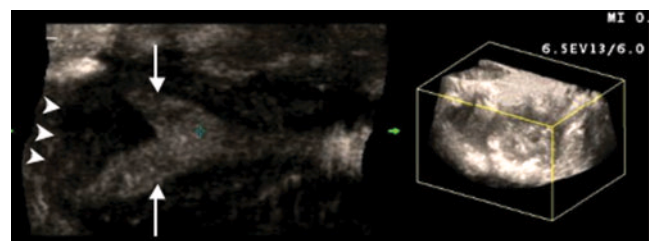
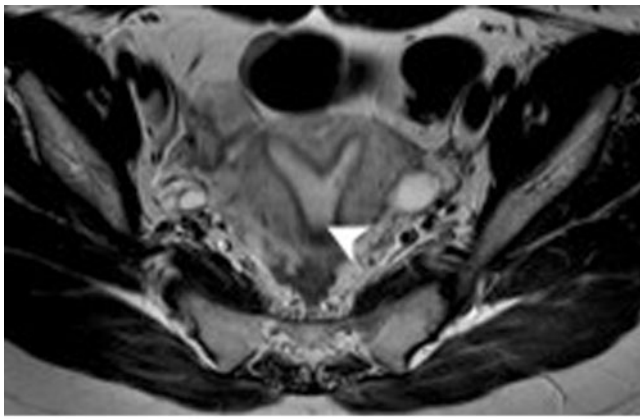
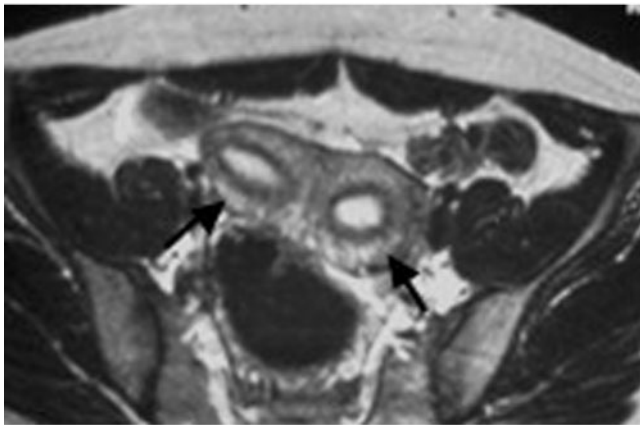


**Figure 9.** A 30-year-old woman with a septate uterus (Class V). A two-dimensional coronal reconstruction (left) of the three-dimensional volume image (right) shows two uterine horns (arrows) and a flat fundal contour (arrowheads).



(a)

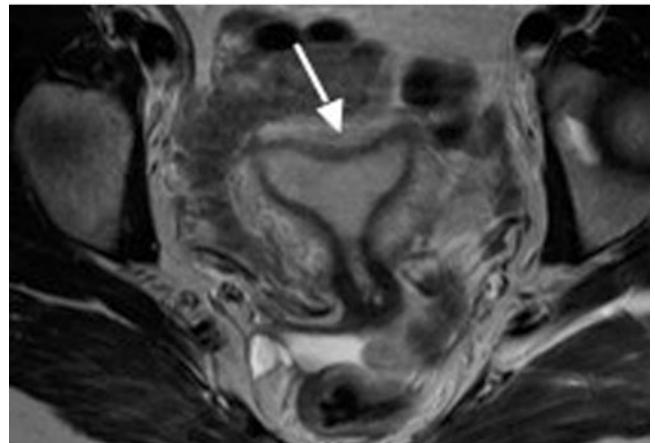


(b)

**Figure 10.** A 25-year-old woman with a septate uterus (Class V) who underwent a spontaneous abortion. (a,b) Subsequent MRI performed on this patient confirms the septate uterus. Axial  $T_2$  weighted image shows two uterine horns (arrows) with incomplete resorption of the midline septum (arrowhead) (a). A faint fibrous segment is seen between the two horns (b).



(a)



(b)

**Figure 11.** Arcuate uterus (Class VI). (a) Hysterosalpingogram of a 36-year-old woman with an arcuate uterus. Note the mild indentation of the endometrium at the uterine fundus (arrow). (b) Axial  $T_2$  weighted MR image of an arcuate uterus in a 28-year-old woman. Note the mild curvature at the fundus (arrow).

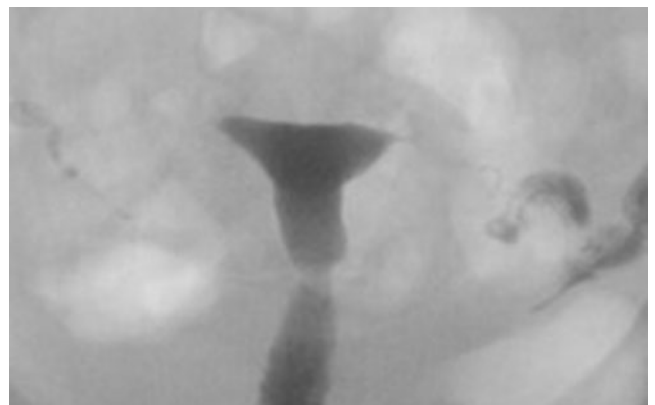
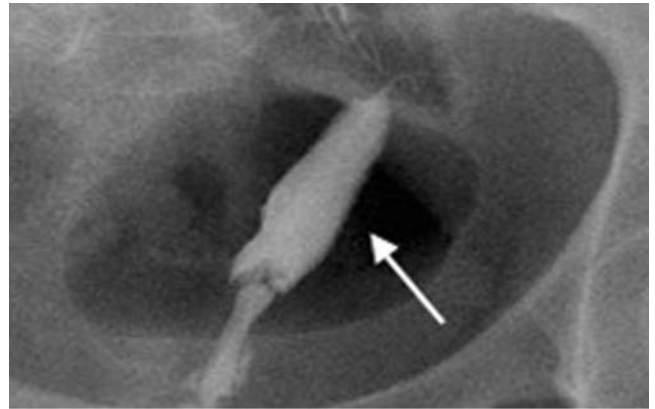


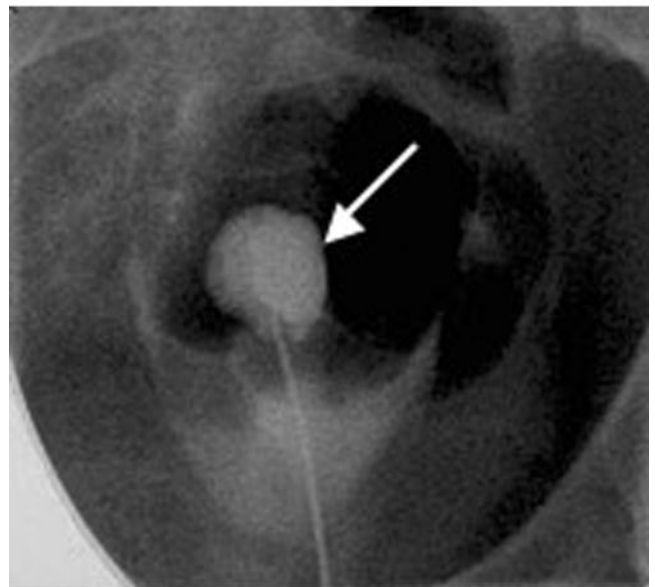
**Figure 12.** A 30-year-old woman with diethylstilbestrol exposure *in utero* (Class VII). Hysterosalpingography illustrates the T-shaped uterus.



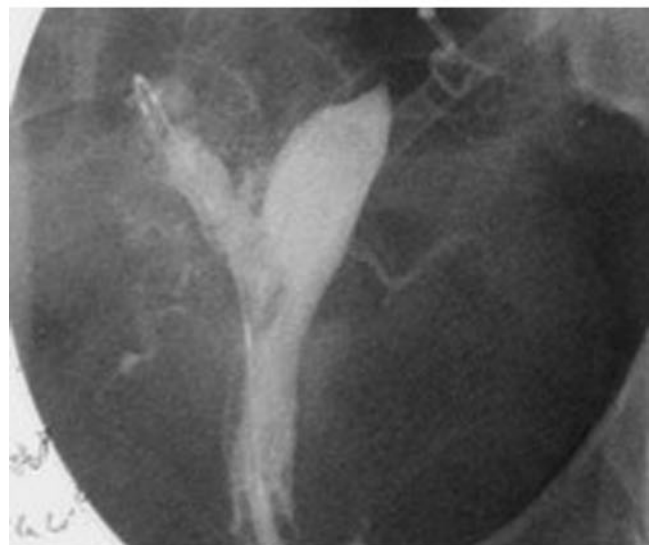
**Figure 13.** A 28-year-old woman with unicornuate uterus and a renal anomaly. This coronal MR image of the retroperitoneum illustrates a congenitally absent left kidney (arrow) in a patient known to have a unicornuate uterus.



(a)



(b)



(c)

**Figure 14.** A 22-year-old with intense menstrual pain who was investigated and found to have a bicornuate uterus with a non-communicating right horn. (a) Hysterosalpingogram reveals filling of the left horn (arrow) but not the obstructed right horn. (b) Intraoperative hysterosalpingogram illustrating the puncture through the uterine septum into the obstructed right horn (arrow). This was performed following needle puncture of the septum with ultrasound guidance. A wire was then placed into the cavity and the gynaecologist then used the wire to guide resection of part of the wall of the obstructing right horn. (c) Subsequent hysterosalpingogram shows filling of the previously obstructed right horn. Note that spasm of the right tube prevented uniform tubal filling. Subsequent selective salpingography demonstrated the right tube to be patent. The patient had resolution of her pain and was very pleased at 2 year follow-up.



performed. Other applications of IR include directing hysteroscopic procedures or dilating occluded structures. For example, where dense synechiae obstruct access to the tubal ostium, a wire can be inserted transvaginally into the fallopian tube to safely direct the hysteroscopic dissection. Likewise, an ultrasound-guided puncture into an occluded endocervical canal followed by balloon catheter angioplasty can be used in cases where standard attempts at cervical dilatation are unsuccessful.

## References

1. The American Fertility Society classifications of adnexal adhesions, distal tubal obstruction, tubal occlusions secondary to tubal ligation, tubal pregnancies, Müllerian anomalies and intrauterine adhesions. *Fertil Steril* 1998;49:944–55.
2. Deutch TD, Abuhamad AZ. The role of 3-dimensional ultrasonography and magnetic resonance imaging in the diagnosis of Müllerian duct anomalies. *J Ultrasound Med* 2008;27:413–23.
3. Mueller GC, Hussain HK, Smith YR, Quint EH, Carlos RC, Johnson TD, et al. Müllerian duct anomalies: comparison of MRI diagnosis and clinical diagnosis. *AJR Am J Roentgenol* 2007;189:1294–302.
4. Heinonen PK, Saarikoski S, Pystynen P. Reproductive performance of women with uterine anomalies: an evaluation of 182 cases. *Acta Obstet Gynecol Scand* 1982; 61:157–62.
5. Homer HA, Li TC, Cooke ID. The septate uterus: a review of management and reproductive outcome. *Fertil Steril* 2000;73:1–14.
6. Herbst AL, Ulferder H, Poskanzer DC. Adenocarcinoma of the vagina: association of maternal stilbesterol therapy with tumour appearance in young women. *N Engl J Med* 1971;284:878–81.
7. Li S, Qayyam A, Coakley FV, Hricak H. Association of renal agenesis and Müllerian duct anomalies. *J Comput Assist Tomogr* 2000;6:829–34.
8. Sanders BH, Machan LS, Gomel V. Complex uterine surgery: a cooperative role for interventional radiology with hysteroscopic surgery. *Fertil Steril* 1998;70:952–5.